

DTIC FILE COPY

CRREL REPORT 88-14

AD-A201 045



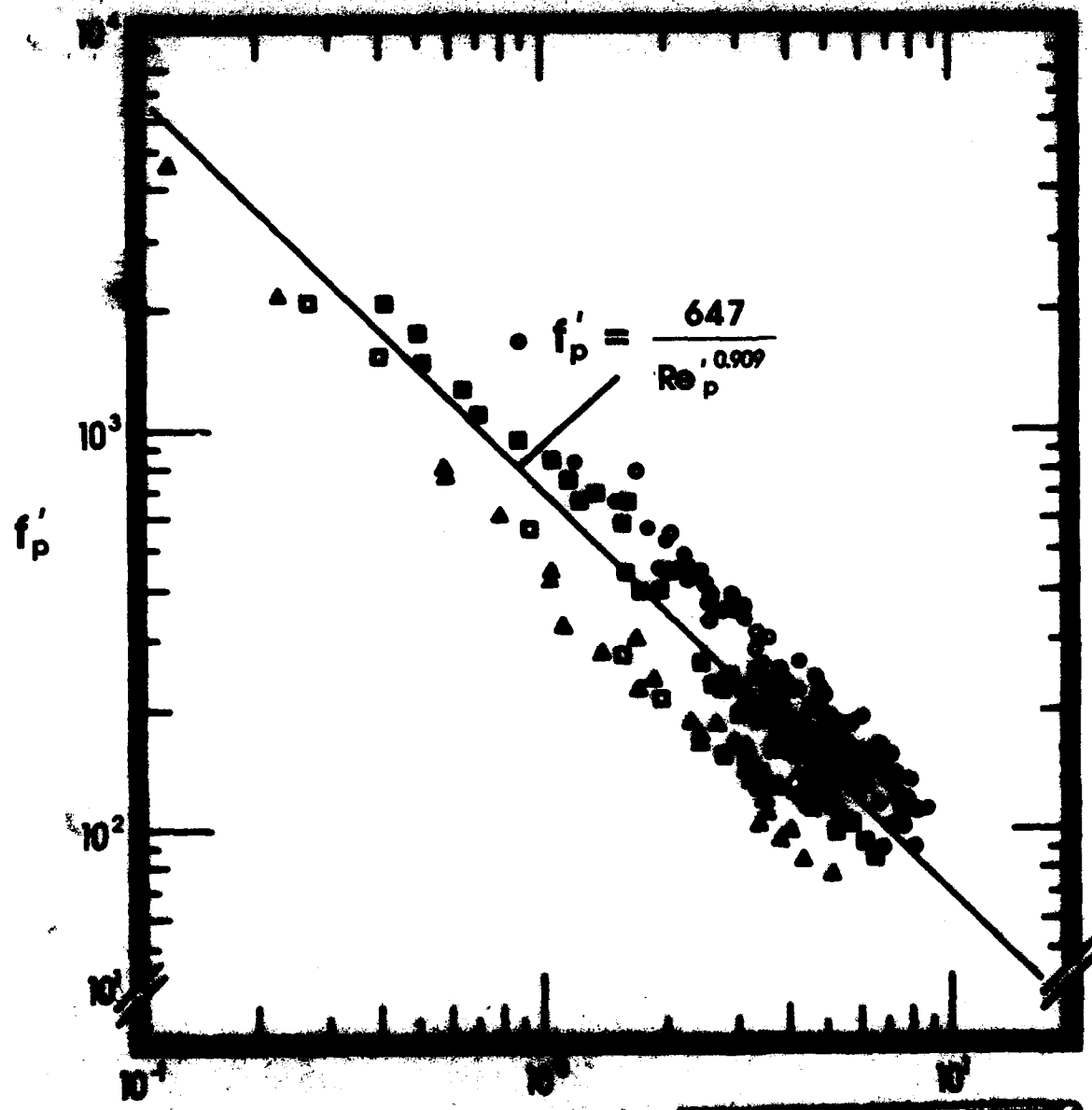
US Army Corps
of Engineers

Cold Regions Research &
Engineering Laboratory

(4)

DTIC
ELECTED
NOV 23 1988
S E D

*On the pressure drop
through a uniform snow layer*



For conversion of SI metric units to U.S./British customary units of measurement consult ASTM Standard E380, Metric Practice Guide, published by the American Society for Testing and Materials, 1916 Race St., Philadelphia, Pa. 19103.

Cover: Relationship between friction factor f_p' and Reynolds number Re'_p (see Fig. 4).

CRREL Report 88-14

September 1988

On the pressure drop through a uniform snow layer

Yin-Chao Yen



Accession For	
NTIS GRA&I <input checked="" type="checkbox"/>	
DTIC TAB <input type="checkbox"/>	
Unannounced <input type="checkbox"/>	
Justification	
By _____	
Distribution/ _____	
Availability Codes	
Dist	Avail and/or
	Special
A-1	

Prepared for
OFFICE OF THE CHIEF OF ENGINEERS

Approved for public release; distribution is unlimited.

88 1122 024

UNCLASSIFIED

SECURITY CLASSIFICATION OF THIS PAGE

Form Approved
OMB No 0704-0188
Exp. Date Jun 30, 1986

REPORT DOCUMENTATION PAGE

1a. REPORT SECURITY CLASSIFICATION Unclassified		1b. RESTRICTIVE MARKINGS	
2a. SECURITY CLASSIFICATION AUTHORITY		3. DISTRIBUTION/AVAILABILITY OF REPORT Approved for public release; distribution is unlimited.	
2b. DECLASSIFICATION/DOWNGRADING SCHEDULE			
4. PERFORMING ORGANIZATION REPORT NUMBER(S) CRREL Report 88-14		5. MONITORING ORGANIZATION REPORT NUMBER(S)	
6a. NAME OF PERFORMING ORGANIZATION U.S. Army Cold Regions Research and Engineering Laboratory	6b. OFFICE SYMBOL (If applicable) CECRL	7a. NAME OF MONITORING ORGANIZATION Office of the Chief of Engineers	
6c. ADDRESS (City, State, and ZIP Code) Hanover, New Hampshire 03755-1290		7b. ADDRESS (City, State, and ZIP Code) Washington, D.C. 20314-1000	
8a. NAME OF FUNDING/SPONSORING ORGANIZATION	8b. OFFICE SYMBOL (If applicable)	9. PROCUREMENT INSTRUMENT IDENTIFICATION NUMBER	
8c. ADDRESS (City, State, and ZIP Code)		10. SOURCE OF FUNDING NUMBERS	
		PROGRAM ELEMENT NO. 6.11.02A	PROJECT NO 4A1611
		TASK NO 02AT24	WORK UNIT ACCESSION NO SS 021
11. TITLE (Include Security Classification) On the Pressure Drop Through a Uniform Snow Layer			
12. PERSONAL AUTHOR(S) Yen, Yin-Chao			
13a. TYPE OF REPORT	13b. TIME COVERED FROM _____ TO _____	14. DATE OF REPORT (Year, Month, Day) September 1988	15. PAGE COUNT 18
16. SUPPLEMENTARY NOTATION <i>Reynolds, Air flow Thermal conductivity Vapor pressure</i>			
17. COSATI CODES		18. SUBJECT TERMS (Continue on reverse if necessary and identify by block number) <i>Fluid flow Friction coefficient Porous media</i>	
FIELD	GROUP	SUB-GROUP	
19. ABSTRACT (Continue on reverse if necessary and identify by block number) <i>An experimental study covering a mass flow rate ranging from 1.62 to 67.45 g/cm²-s and snow density varying from 0.377 to 0.472 g/cm³ has been conducted. Pressure drops ranging from 0.012 to 2.868 gf/cm² were recorded. A plot of the friction factor f_p vs Re (defined as the classical Reynolds number Re for fluid flow through conduits) showed a good representation of all the experimental data. The least-squares analysis resulted in an expression of f_p = 118/Re^{1.095} for snow, in comparison with the expression f_p = 64/Re developed for fluid flow through porous media of randomly packed metallic and nonmetallic materials of spherical and nonspherical shapes.</i>			
20. DISTRIBUTION/AVAILABILITY OF ABSTRACT <input checked="" type="checkbox"/> UNCLASSIFIED/UNLIMITED <input type="checkbox"/> SAME AS RPT <input type="checkbox"/> DTIC USERS		21. ABSTRACT SECURITY CLASSIFICATION Unclassified	
22a. NAME OF RESPONSIBLE INDIVIDUAL Yin-Chao Yen		22b. TELEPHONE (Include Area Code) 603-646-4100	22c. OFFICE SYMBOL CECRL-EC

PREFACE

This report was prepared by Dr. Yin-Chao Yen, Research Physical Scientist, of the Civil and Geotechnical Engineering Research Branch, Experimental Engineering Division, U.S. Army Cold Regions Research and Engineering Laboratory. Funding for this research was provided by D.A. Project 4A161102AT24, *Research in Snow, Ice and Frozen Ground, Task SS, Properties of Cold Regions Materials, Work Unit 021, Synopsis of Cold Regions Environmental Heat Transfer.*

Dr. Virgil Lunardini and Dr. Yoshisuke Nakano of CRREL technically reviewed the manuscript of this report.

The contents of this report are not to be used for advertising or promotional purposes. Citation of brand names does not constitute an official endorsement or approval of the use of such commercial products.

CONTENTS

	Page
Abstract	i
Preface	ii
Nomenclature	iv
Introduction	1
Experimental setup and procedure	2
Experimental results	3
Discussion and conclusions	9
Literature cited	10

ILLUSTRATIONS

Figure

1. Schematic of the experimental setup.....	3
2. Pressure drop due to friction losses as a function of mass flow rate G	4
3. Relationship between friction factor f_p and Reynolds number Re_p	8
4. Relationship between friction factor f'_p and Reynolds number Re'_p	8

TABLES

Table

1. Summary of derived parameters as a function of snow density.....	4
2. Coefficients a and b and correlation coefficient γ	5
3. Summary of experimental results and calculated data.....	6

NOMENCLATURE

<i>a</i>	constant in eq 16
<i>A</i>	cross-sectional area
<i>b</i>	fissure width, also constant in eq 16
<i>B</i>	constant in eq 6, 7 and 8
<i>a + b</i>	fissure-to-fissure spacing
<i>d</i>	diameter of sphere
<i>D</i>	diameter of conduit
<i>D_p</i>	nominal particle diameter
<i>f</i>	friction factor defined as $2g_c D(-\Delta p)_f \varrho / LG^2$
<i>f_p</i>	friction factor for porous media defined as $\frac{2g_c D(-\Delta p)_f \varrho}{F_f LG^2}$
<i>f'_p</i>	friction factor defined in eq 18
<i>F_f</i>	friction factor coefficient
<i>F_{Re}</i>	Reynolds number factor
<i>g</i>	gravitational constant
<i>g_c</i>	conversion factor
<i>G</i>	mass flow rate
<i>L</i>	sample length
<i>Iw_f</i>	frictional losses per unit mass
<i>N</i>	number of tubes, in cross-sectional area <i>A</i>
<i>p</i>	pressure
$(-\Delta p)_f$	pressure drop due to friction losses
<i>r_o</i>	radius of capillary tube
<i>Re</i>	Reynolds number defined as $D\varrho u/\mu$
<i>Re_l</i>	local pore Reynolds number
<i>Re_p</i>	Reynolds number for porous media defined as $D_p \varrho v F_{Re} / \mu$
<i>Re'</i>	Reynolds number defined in eq 19
<i>x, y, z</i>	Cartesian coordinates
<i>u</i>	velocity component in <i>x</i> -direction
<i>v</i>	velocity component in <i>y</i> -direction
<i>w</i>	velocity component in <i>z</i> -direction
μ	viscosity
ϱ	density
ϵ, ϵ_0	porosity, highest porosity
δ	surface roughness
γ	correlation coefficient
ψ	sphericity

On the Pressure Drop Through a Uniform Snow Layer

YIN-CHAO YEN

INTRODUCTION

Fluid flow through a bed of contiguous particles is distinct from the flow through a conduit. Since its passage is between the particles of the bed, the flow is dependent upon the porosity of the bed or column and diameter, sphericity, orientation and roughness of the particles. The actual linear velocity of the fluid through the passages in the porous medium may be expressed in terms of "superficial" velocity (computed as the rate of flow of fluid through the entire undisturbed cross-sectional area of the bed).

The most frequently used model for volume-averaged flow through a porous medium is Darcy's flow model. In one-dimensional flow, it can be expressed by

$$u = \frac{K}{\mu} \frac{\partial p}{\partial x} \quad (1)$$

where u = velocity component in x -direction

K = permeability of the medium

μ = viscosity

p = pressure.

For three-dimensional flow in the presence of a gravitational acceleration vector \mathbf{g} (g_x, g_y, g_z), eq 1 can be written as

$$\mathbf{v} = \frac{K}{\mu} (-\nabla p + \rho \mathbf{g}) \quad (2)$$

where \mathbf{v} is the velocity vector, ρ is density and K , usually expressed in units of length squared (i.e. m^2 , cm^2 , or ft^2), can be determined by measuring the pressure drop and the flow rate. Considering the pores as a bundle of parallel capillary tubes of radius r_0 or the pores as a stack of parallel capillary fissures of width b and fissure-to-fissure spacing $a+b$, Bear (1972) derived the following expressions:

$$K = \frac{\pi r_0^4 N}{8A} \quad (3)$$

and

$$K = \frac{b^3}{12(a+b)} \quad (4)$$

where N is the number of tubes contained on a cross section of area A .

Kozeny (1927), on the other hand, considered the porous medium as a collection of solid spheres and arrived at the following permeability expression:

$$K \sim \frac{d^2 \epsilon^3}{(1-\epsilon)^2} \quad (5)$$

where ϵ is the porosity (the ratio of void volume to the total volume of the porous medium), and d is the diameter of the spheres. Darcy's flow model is believed to be valid as long as the so-called local pore Reynolds number Re_l based on local volume-averaged speed [i.e. $(u^2 + v^2 + w^2)^{1/2}$] and $K^{1/2}$ are smaller than one. For Re_l greater than one, modification of this model has been proposed by Ferschheimer (1901) as

$$-\frac{\partial p}{\partial x} = \frac{\mu}{K} u + B \rho u^2. \quad (6)$$

For three dimensions and in the presence of body acceleration, this modification becomes

$$\mathbf{v} + \frac{BeK}{\mu} \cdot \mathbf{v} \cdot \mathbf{v} = \frac{K}{\mu} (-\nabla p + \rho \mathbf{g}). \quad (7)$$

Ward (1964) suggested the value of B as

$$B = -0.55 K^{1/2}. \quad (8)$$

for Re_l exceeding approximately 10. Ergum (1952),

after conducting extensive measurements on gas flow through columns of packed spheres, sands and pulverized coal, provided the correlations for K and B as

$$K = \frac{d^2 \epsilon^3}{150(1-\epsilon)^2} \quad (9)$$

and

$$B = \frac{1.75(1-\epsilon)}{d\epsilon^3} \quad (10)$$

The loss due to friction accompanying the flow through porous media can be derived from expressions used for fluid flow through conduits such as

$$f = \frac{2g_c D l w_f}{L v^2} = \phi \left[\left(\frac{\delta}{D} \right) \left(\frac{D \rho u}{\mu} \right) \right] \quad (11)$$

where f = frictional loss factor

g_c = conversion factor (32.17 poundals per pound in English units)

D = diameter of the conduit

L = length of the conduit

$l w_f$ = frictional energy loss per unit mass

δ = surface roughness

u = superficial velocity, i.e. a linear velocity computed on the basis of the total crosssectional area.

In the case of fluid flow through a porous medium, the Reynolds number will be modified to

$$Re_p = \frac{D_p \rho u F_{Re}}{\mu} \quad (12)$$

where D_p is the diameter of the particle, F_{Re} is a factor dependent on the value of porosity ϵ and sphericity ψ (which is defined as the area of the sphere having the same volume as the particle divided by the area of the particle) of the medium. The friction factor f_p is adjusted to include a factor F_f also dependent on the values of ϵ and ψ as

$$f_p = \frac{2g_c D_p l w_f}{L v^2 F_f} = \frac{2g_c D_p (-\Delta p)_f \rho}{F_f L G^2}. \quad (13)$$

When all particles are of the same size, the screen size (D_{avg}) may be used. For mixed sizes, D_p is the mean surface diameter given by

$$D_p = \left[\frac{\sum M_i / D_i}{\sum M_i / D_i^2} \right]^{1/2} \quad (14)$$

where M_i is the mass fraction of a given particle size and D_i is the diameter of particles in each size fraction taken as the arithmetic average of the screen openings passing and retaining the particles. The value of F_{Re} and F_f can be evaluated from the graph given in Brown et al. (1953) and presented as functions of ϵ and ψ . The porosity is closely related to the sphericity. However, different porosities are expected with particles of the same shape through variations in spatial arrangement. Consequently both porosity and sphericity are required to define the porous medium. Although the sphericity could theoretically be calculated from the dimensions of the particle, this is often difficult or virtually impossible for randomly packed beds of uniform-sized particles. The sphericity is found to be a unique function of porosity with a slight variation due to the nature of packing (i.e. loose, normal or dense).

EXPERIMENTAL SETUP AND PROCEDURE

The test apparatus is identical to the one used in determining the effective thermal conductivity and water vapor diffusivity of the snow (Yen 1962, 1963). Figure 1 is a schematic of the experimental setup. The entire apparatus, with the exception of the manometer, the wet-test meter (to measure the air flow rate) and the Leeds and Northrup potentiometer (placed in the adjacent corridor maintained at ordinary room temperature), was situated in a refrigerated room kept at approximately -20°C. Coldroom air was compressed and then passed through a tank to minimize the fluctuations of the air pressure. A pancake-type pressure regulator was used to obtain the desired flow rate. Since the coldroom could only be maintained to within ± 1°C, the air was passed through a constant temperature bath where the temperature could be maintained at slightly above room temperature to an accuracy of ± 0.05°C.

The Dewar flask, 6.5 cm I.D., 15.24 cm in height and made of double-walled glass tubing with the annular space being evacuated and the internal surface plated with silver, contained the snow sample and was enclosed in an aluminum casing equipped with a flange at both ends. The casing was made so that the flask fitted tightly into it, and the flask was coated with a low-temperature silicone grease before assembly to prevent any possible air leakage. As soon as a steady state was established, the water temperature at the wet-test meter was recorded with a Rubican potentiometer

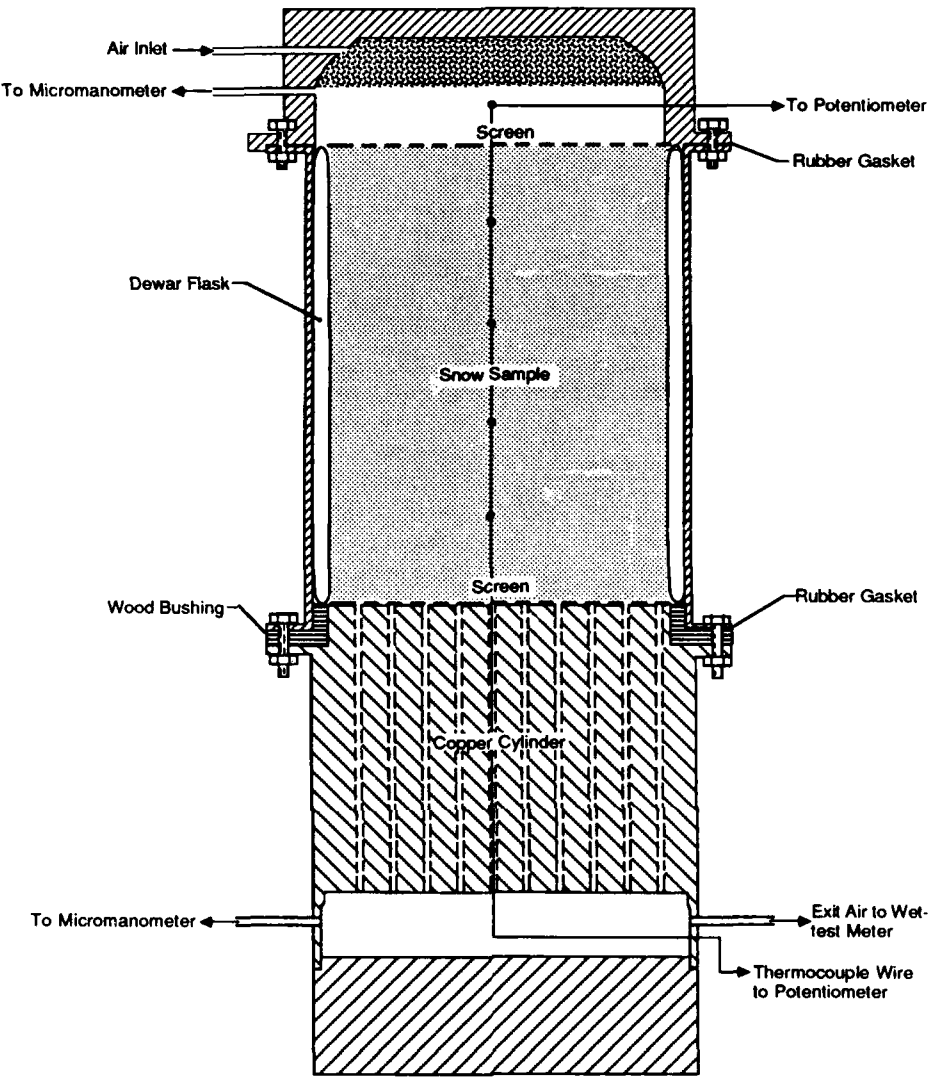


Figure 1. Schematic of the experimental setup.

accurate to $\pm 0.05^\circ\text{C}$ along with the absolute barometric pressure. The wet-test meter was checked by the standard displacement method and was found to be accurate within 20 cm^3 out of 3000 cm^3 ($\pm 0.7\%$). The displacement capacity of the meter is 300 cm^3 per revolution with 300 divisions on the dial. The snow samples for the experiments covered a range of sieve numbers, 5-10, 10-12, 14-16, 18-20 and 25-30, with corresponding nominal snow particle diameters of 0.219, 0.182, 0.129, 0.092 and 0.065 cm, respectively. The snow sample density was determined by recording the

amount of snow poured into the flask to be flush with the sample container (i.e. ρ_s = weight of snow/volume of the sample container). Several determinations were made for all the specific sieve fractions and an arithmetic average snow density was determined.

EXPERIMENTAL RESULTS

A great number of experimental runs were conducted for each snow density covered in the study.

Table 1. Summary of derived parameters as a function of snow density.

Snow density, ρ_s (g/cm ³)	Snow porosity, ϵ	Snow particle diameter, D_p (cm)	Sphericity of snow particle, ψ	Reynolds number factor, F_{Re}	Friction coefficient, F_f
0.377	0.589	0.219	0.55	43.5	830
0.387	0.578	0.182	0.55	45.0	950
0.427	0.534	0.129	0.60	47.0	1150
0.447	0.512	0.092	0.65	47.0	1150
0.472	0.485	0.065	0.70	47.0	1150

Table 1 summarizes the derived parameters as function of snow density. The porosity ϵ is evaluated as

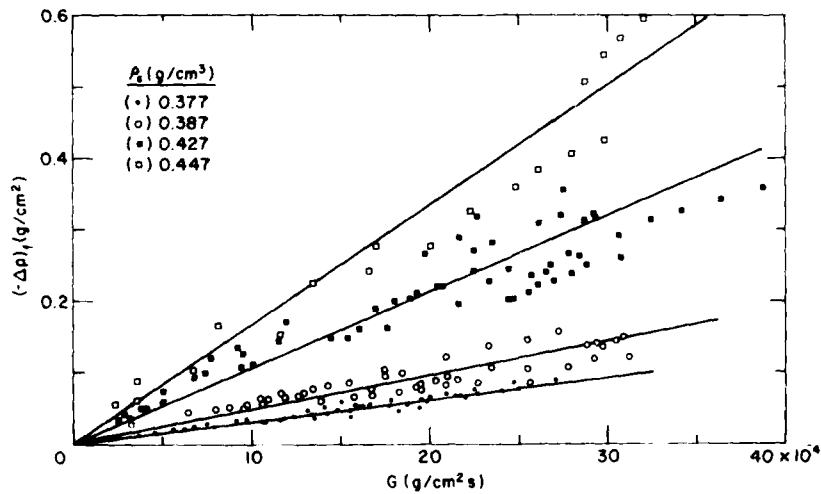
$$\epsilon = \frac{\rho_i - \rho_s}{\rho_i} \quad (15)$$

where ρ_i is the ice density, usually taking a value of 0.917 g/cm³. The snow particle nominal diameter D_p was evaluated by arithmetically averaging the two sieve openings. The sphericity ψ , Reynolds number factor F_{Re} and coefficient F_f are taken from the graphs given in Brown et al. (1953). Since the snow density has only slightly more than 25% variation, there is merely a weak variation at the most in values of ψ and F_{Re} . However, the values of F_f were rather sensitive to the changes of ϵ and

ψ . Figures 2a and b show the variation of pressure drop ($-\Delta p_f$) vs the mass flow rate G (g/cm²s). It can be seen that under the combination of experimental conditions (i.e. for the range of snow density and the variation of the mass flow rate covered in this study) a linear relationship exists between $(-\Delta p_f)$ and G . The coefficients a and b of the linear expression

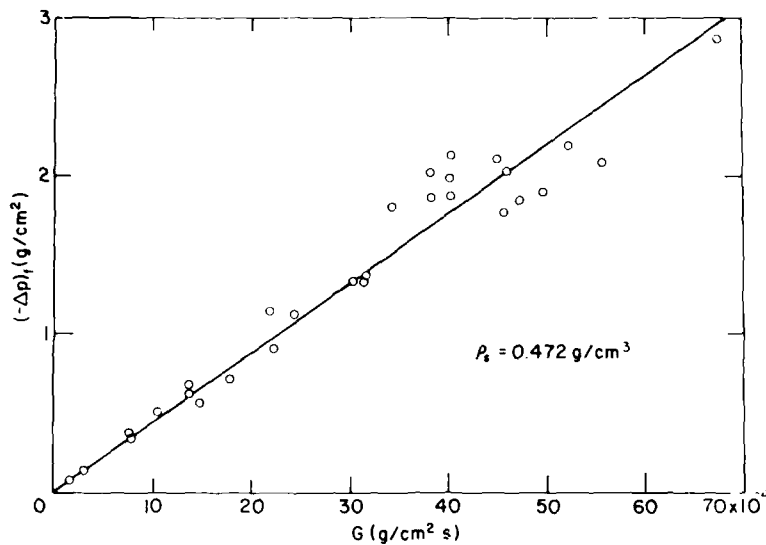
$$(-\Delta p_f) = a + b G \times 10^{-4} \quad (16)$$

were determined from least-squares analysis and are summarized in Table 2 along with the correlation coefficients. Theoretically, the values of a should be zero, and small values of a are indicative of the accuracy of the experimental measurement. However, for practical purposes, one can hardly



a. For $\rho_s = 0.377, 0.387, 0.427$ and 0.447 g/cm³.

Figure 2. Pressure drop due to friction losses as a function of mass flow rate G .



b. For $\rho_s = 0.472 \text{ g/cm}^3$.

Figure 2 (cont'd).

Table 2. Coefficients a and b in $(-\Delta p)_f = a + bG \times 10^{-4}$ and correlation coefficient γ .

Snow density, ρ_s (g/cm³)	Coefficient		Correlation coefficient, γ
	a (gf*/cm²)	b (gf·s/g)	
0.377	3.671×10^{-4}	31.267	0.9492
0.387	1.582×10^{-3}	39.382	0.8130
0.427	3.137×10^{-3}	88.425	0.8681
0.447	8.854×10^{-3}	176.95	0.9933
0.472	8.478×10^{-3}	413.20	0.9504

* gf—gram-force.

detect that the lines in Figures 2a and b do not pass through the origin.

Table 3 summarizes the experimental data and the calculated values of Re_p (defined as $D_p G F_{Re}/\mu$) and friction factor f_p [defined in eq 15 as $f_p = 2g_c D_p (-\Delta p)_f \rho / F_f L G^2$]. An average value of μ based on the arithmetic mean of the inlet and outlet air temperature was used. The mass flow rate was determined on the basis of the exit air temperature and the prevailing atmospheric pressure. Figure 3 shows the variation of f_p versus Re_p . The results of a least-squares analysis of the results can be expressed by

$$f_p = \frac{118}{Re_p^{1.095}} \quad (17)$$

with a rather high correlation coefficient of 0.9688. Equation 17 gives a value of f_p approaching that of $f_p = 65/Re_p$ as Re_p approaches the limit of the laminar flow region (say $Re_p = 400$) recommended for randomly packed particles (metallic or nonmetallic cylinders, rings, spheres, etc.).

Another way to represent the experimental results is by expressing the friction factor f'_p and the Reynolds number Re'_p , respectively, by

$$f'_p = \frac{f_p F_f \epsilon^3}{2(1-\epsilon)} \quad (18)$$

and

$$Re'_p = \frac{Re_p}{F_{Re}(1-\epsilon)} \quad (19)$$

The least-squares analysis of f'_p and Re'_p can be represented by

$$f'_p = \frac{Re_p}{Re_p'^{0.909}} \quad (20)$$

but only with a moderate correlation coefficient of 0.8385. Figure 4 shows a plot of f'_p vs Re'_p , and it can be clearly seen that the value f'_p has a weak dependence on the snow density or porosity.

Table 3. Summary of experimental results and calculated data.

$G \times 10^{-4}$ ($g/cm^2 s$)	$(-\Delta p)_f$ (gf/cm^2)	Re ($D_p F_{Re} G / \mu$)	f_p $[2g_c D_p (-\Delta p)_f \varrho / F_f LG]$	$G \times 10^{-4}$ ($g/cm^2 s$)	$(-\Delta p)_f$ (gf/cm^2)	Re ($D_p F_{Re} G / \mu$)	f_p $[2g_c D_p (-\Delta p)_f \varrho / F_f LG]$
$\varrho_s = 0.377 \text{ g/cm}^3, D_p = 0.219 \text{ cm}$							
13.11	0.048	75.1	1.28	16.73	0.069	82.7	0.82
14.02	0.051	80.3	1.19	19.43	0.075	95.9	0.66
9.11	0.032	52.2	1.77	20.94	0.096	103.5	0.73
7.57	0.027	43.3	2.16	25.50	0.118	144.5	0.46
15.09	0.051	86.4	1.03	31.16	0.105	126.2	0.54
16.20	0.053	92.8	0.92	20.92	0.083	154.2	0.42
17.80	0.062	102.0	0.90	25.65	0.081	103.4	0.63
19.52	0.062	112.0	0.74	8.77	0.051	125.9	0.41
24.70	0.085	142.1	0.64	9.67	0.051	43.2	2.21
27.09	0.088	155.7	0.55	10.73	0.061	47.6	1.81
25.09	0.078	144.2	0.57	12.59	0.068	52.9	1.77
22.68	0.070	130.4	0.62	30.93	0.150	62.1	1.43
21.47	0.068	123.5	0.68	29.72	0.135	153.0	0.52
19.98	0.067	114.9	0.77	21.50	0.091	147.1	0.51
5.66	0.019	32.4	2.72	20.26	0.089	106.3	0.66
9.70	0.033	55.6	1.61	19.46	0.083	0.72	0.73
11.63	0.034	66.6	1.15	19.33	0.081	95.5	0.72
14.14	0.041	81.0	0.94	18.33	0.077	90.6	0.76
15.82	0.052	90.9	0.95	16.84	0.072	83.2	0.85
19.77	0.057	113.5	0.67	15.94	0.066	78.8	0.86
21.75	0.068	124.8	0.66	27.80	0.106	137.6	0.46
24.02	0.075	137.9	0.59	22.72	0.088	112.3	0.57
21.91	0.066	125.9	0.63	17.50	0.102	86.0	1.11
10.61	0.031	60.9	1.26	20.93	0.123	86.5	0.94
3.71	0.012	21.3	4.00	23.27	0.137	115.0	0.84
6.84	0.024	39.1	2.35	25.54	0.145	126.3	0.74
16.60	0.058	95.0	0.96	27.27	0.157	134.9	0.70
17.70	0.055	101.3	0.80	11.75	0.070	57.8	1.69
20.93	0.070	119.8	0.73	14.24	0.083	70.2	1.36
22.57	0.075	129.1	0.67	15.41	0.085	71.5	1.19
16.02	0.051	91.7	0.91	17.52	0.096	86.2	1.04
14.70	0.047	84.0	1.00	18.20	0.100	89.8	1.01
13.29	0.042	75.9	1.08	6.39	0.044	31.5	3.60
18.36	0.054	105.2	0.73	8.00	0.048	39.4	2.50
6.23	0.022	35.7	2.60	10.43	0.063	42.8	1.93
7.86	0.024	45.1	1.78	11.89	0.065	48.8	1.53
10.70	0.029	61.5	1.16	3.39	0.026	16.7	7.56
12.34	0.038	70.9	1.14	13.41	0.076	66.1	1.41
15.45	0.047	89.0	0.90	$\varrho_s = 0.427 \text{ g/cm}^3, D_p = 0.129 \text{ cm}$			
11.70	0.035	67.3	1.17				
4.66	0.015	26.7	3.17	3.84	0.050	14.1	6.63
13.36	0.037	76.9	0.95	16.95	0.190	62.5	1.29
15.54	0.038	89.4	0.72	9.48	0.107	34.9	2.33
18.20	0.046	104.9	0.64	4.11	0.050	15.1	5.77
19.39	0.051	111.8	0.62	5.00	0.059	18.3	4.61
$\varrho_s = 0.387 \text{ g/cm}^3, D_p = 0.182 \text{ cm}$							
9.70	0.053	47.8	1.88	2.48	0.034	9.1	10.82
10.69	0.056	52.7	1.63	18.04	0.201	66.6	1.21
12.92	0.070	63.8	1.40	10.16	0.110	37.4	2.08
28.83	0.137	142.7	0.55	24.38	0.246	90.1	0.81
29.43	0.142	145.6	0.55	16.02	0.160	59.1	1.22
30.48	0.144	150.9	0.52	2.91	0.041	10.7	9.47
23.49	0.107	116.2	0.65	28.43	0.262	105.0	0.63
13.89	0.060	68.8	1.04	26.52	0.240	98.1	0.67
				21.64	0.198	79.9	0.83
				11.54	0.144	42.5	2.11
				7.39	0.099	27.1	3.55

Table 3 (cont'd).

$G \times 10^{-4}$ ($g/cm^2 \cdot s$)	$(-\Delta p)_f$ (gf/cm^2)	Re ($D_p F_{Re} G / \mu$)	f_p $[2g_c D_p (-\Delta p)_f c / F_f L G]^1/2$	$G \times 10^{-4}$ ($g/cm^2 \cdot s$)	$(-\Delta p)_f$ (gf/cm^2)	Re ($D_p F_{Re} G / \mu$)	f_p $[2g_c D_p (-\Delta p)_f c / F_f L G]^1/2$
5.02	0.074	18.4	5.73				
9.52	0.127	35.0	2.74				
29.18	0.319	107.8	0.73				
22.57	0.243	83.3	0.93	2.38	0.053	6.2	13.05
19.32	0.211	71.2	1.11	3.59	0.089	9.3	9.62
34.16	0.327	126.3	0.55	8.00	0.166	20.8	3.60
30.59	0.290	113.0	0.61	32.03	0.599	83.8	0.81
27.75	0.265	102.5	0.67	30.71	0.566	80.3	0.83
14.43	0.149	53.2	1.40	29.87	0.544	78.2	0.84
15.43	0.150	56.9	1.23	28.64	0.507	75.0	0.86
25.50	0.212	94.2	0.64	24.82	0.425	64.9	0.96
26.98	0.226	99.7	0.61	13.34	0.224	34.8	1.75
24.68	0.202	91.2	0.65	16.93	0.281	44.2	1.37
6.90	0.096	25.4	3.94				
22.68	0.321	83.8	1.22				
9.19	0.135	33.8	3.12				
11.91	0.172	43.9	2.37	7.79	0.379	14.3	6.13
7.98	0.121	29.4	3.71	13.68	0.667	25.2	3.50
19.77	0.266	73.0	1.33	24.30	1.120	44.8	1.86
21.74	0.290	80.3	1.20	13.70	0.617	25.2	3.23
27.53	0.357	101.8	0.92	22.31	0.909	41.1	1.79
22.46	0.271	83.0	1.05	14.60	0.553	26.9	2.55
23.41	0.283	86.5	1.01	2.84	0.140	5.2	17.06
26.10	0.310	96.6	0.89	1.62	0.098	3.0	36.89
27.37	0.320	101.3	0.84	21.78	1.142	40.2	2.36
28.64	0.311	106.0	0.74	34.31	1.755	63.5	1.46
29.31	0.316	108.5	0.72	40.89	2.122	75.7	1.25
32.42	0.313	120.1	0.58	40.75	2.016	75.4	1.19
36.38	0.340	134.8	0.50	38.14	1.871	70.6	1.26
38.82	0.358	144.0	0.46	10.41	0.526	19.1	4.77
26.10	0.221	96.6	0.63	44.89	2.098	83.1	1.02
20.61	0.219	76.2	1.01	42.66	1.976	79.0	1.07
3.02	0.035	11.1	7.50	40.72	1.868	75.4	1.11
18.97	0.202	70.1	1.10	7.65	0.364	14.1	6.10
20.60	0.220	76.2	1.01	45.72	2.020	84.7	0.95
23.36	0.228	86.4	0.82	30.26	1.320	56.0	1.42
17.68	0.164	65.3	1.03	31.10	1.326	57.5	1.35
25.68	0.236	95.1	0.70	31.58	1.348	58.4	1.33
26.73	0.248	99.0	0.68	67.45	2.862	125.2	0.62
28.09	0.238	104.0	0.59	52.32	2.175	97.1	0.78
28.82	0.250	106.7	0.59	17.90	0.710	33.0	2.18
30.94	0.258	114.5	0.53	47.02	1.828	87.1	0.81
24.60	0.201	91.0	0.65	45.59	1.753	84.5	0.83
				49.67	1.879	92.0	0.75
				55.40	2.066	102.8	0.66

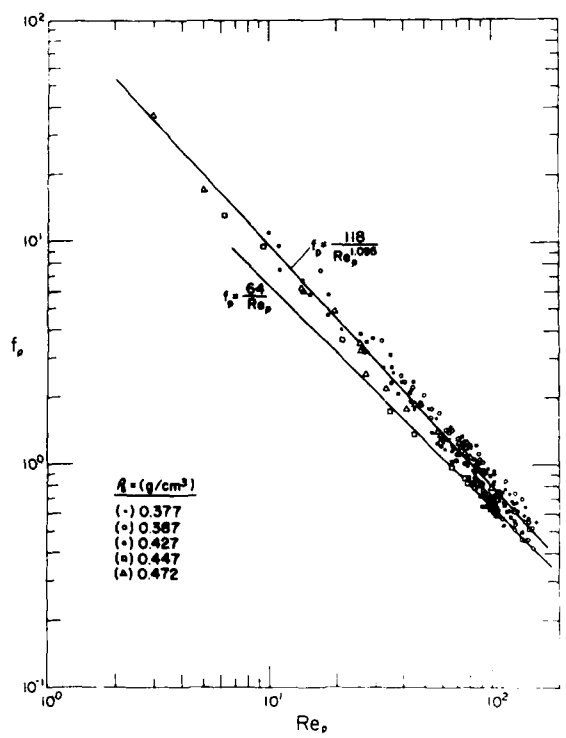


Figure 3. Relationship between friction factor f_p and Reynolds number Re_p .

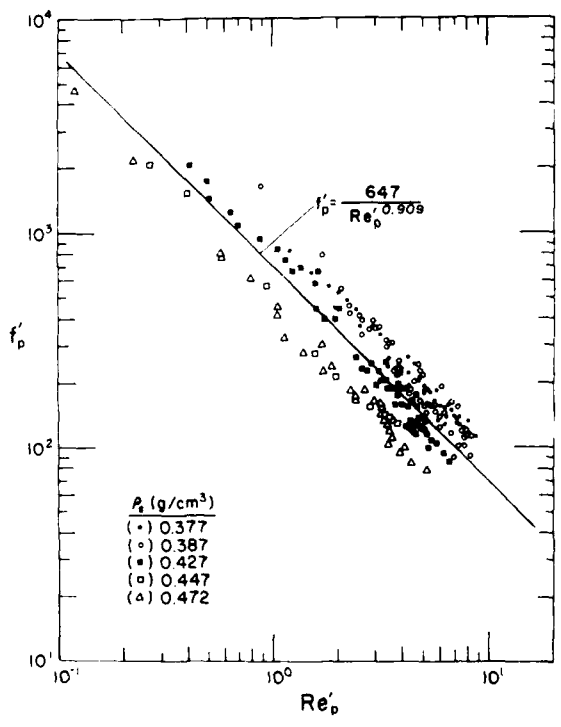


Figure 4. Relationship between friction factor f'_p and Reynolds number Re'_p .

DISCUSSION AND CONCLUSIONS

As shown in Table 2, the pressure drop through the snow layer for snow with density ranging from 0.377 to 0.472 g/cm³ can be fairly well represented linearly with the superficial mass flow rate G . The least-squares analysis for each snow density resulted in correlation coefficients from a moderate value of 0.8130 to a rather high value of 0.9933. From Figure 3, it can be seen that the air flow encounters higher resistance through snow as compared to gas flow through randomly packed porous columns of metallic and nonmetallic spherical and nonspherical materials (in the latter case, there was no phase change or mass transport accompanying the flow). Since snow is very sensitive to temperature, its physical properties are constantly changing through metamorphism, which creates ice bonds among the snow grains even under isothermal conditions through the process of sintering.

Since the experiment was set up to evaluate the thermal conductivity and vapor diffusivity of the snow, a moderate temperature gradient was imposed, even though the air entering at the top of the column was saturated to prevent or to limit the mass transport between the snow grains and the fluid stream as it flowed through the interconnected pores. Though a thermal equilibrium is assumed between the snow grain and the air stream as it passes the grain surface, the air still picks up the water vapor as it flows downward and comes into contact with snow, which was maintained at higher temperature at the exit. The moist snow must exhibit more drag or stickiness to the air flow than the dry and rather smooth surfaces of metallic and nonmetallic surfaces.

In laminar flow, equations of the same form may be used for the friction loss through the porous medium as for the fluid flow through the conduits (i.e. the pressure drop due to friction losses through a porous medium) is

$$(-\Delta p)_f = \frac{32Lv\mu F_f}{g_c D_p^2 F_{Re}} = \varrho / w_f \quad (21)$$

and for flow through a conduit is

$$(-\Delta p)_f = \frac{32Lv\mu}{g_c D^2} = \varrho / w_f. \quad (22)$$

In both flows, the friction factor can be represented by

$$f_p = \frac{64}{Re_p} , \quad f = \frac{64}{Re}. \quad (23)$$

The only difference between f_p , Re_p and f , Re is that f_p and Re_p contain factors of F_f and F_{Re} , respectively, in addition to the parameters used in defining f and Re . By rewriting eq 21, i.e. by solving for velocity u , it follows that

$$u = \frac{g_c D_p^2 F_{Re}}{32 F_f} \frac{\varrho / w_f}{L \mu} = K \frac{\varrho / w_f}{L \mu} \quad (24)$$

in which K is the air permeability of snow used in eq 1, i.e.

$$K = \frac{g_c D_p^2 F_{Re}}{32 F_f}. \quad (25)$$

From this, the value of K can be calculated without performing an experiment, if the dimensionless factors F_{Re} and F_f and the particle dimensions are known. The value of K is directly proportional to D_p^2 but implicitly K depends on porosity and sphericity through the factors of F_{Re} and F_f .

Bender (1957) reported an extensive study on air permeability of snow and pointed out that the air flow is laminar for velocities of less than 5 cm/s for fine-grained snow (less than 0.8 mm in diameter); 2 cm/s for medium-grained snow (0.8 to 1.2 mm in diameter); and 1 cm/s for large-grained snow. He reported that all of his results, as long as the flow is in laminar region, can be represented by a single relationship, i.e.

$$K = \frac{16.8 D_p^{1.63} \epsilon / \epsilon_0}{\epsilon_0 - \epsilon} \quad (26)$$

where K = air permeability expressed in cm/s

D_p = average snow grain size in mm

ϵ_0 = highest porosity (i.e. when the packing is in loosest state) attainable for the given shape of the snow particle.

Since no specific experimental data were given in terms of pressure gradient, volumetric flow rate or superficial velocity, or porosities ϵ and ϵ_0 , it was not possible to compare the results from eq 25 and 26. Furthermore, snow is so sensitive to the temperature and aging through metamorphism that it will be indeed difficult to reproduce experimental results even if identical samples and measurement techniques are used.

It can be concluded from this study that the pressure drop or friction loss of air flow through a uniform snow layer can be correlated in terms of f_p and Re_p with a high correlation coefficient (0.9688) or in modified form of f'_p and Re'_p with a moderate correlation coefficient of 0.8385. In view of the complex processes of mass exchange and physical structure transformation taking place even under isothermal conditions, the results presented should provide useful information in predicting energy requirements for air to penetrate a uniform snow layer of various snow densities.

LITERATURE CITED

Bear, J. (1972) *Dynamics of Fluid in Porous Media*. New York: American Elsevier.

- Bender, J.A.** (1957) Air permeability of snow. USA Snow, Ice and Permafrost Research Establishment, Research Report 37. AD 158 193.
- Brown, G.G. et al.** (1913) *Unit Operations*. New York: John Wiley & Sons, fourth printing.
- Ergun, S.** (1952) Fluid flow through packed columns. *Chemical Engineering Progress*, **48**(2): 89-94.
- Forschheimer, P.H.** (1901) *Zeitschrift Ver. Dtsch. Ing.*, **45**: 1782-1788.
- Kozeny, J.** (1927) Über kapillare Leitung des Wassers in Boden Sitzber. Akad. Wiss. Wien, *Math-Naturw. Kl.*, vol. 136, Abt IIa, p. 277.
- Yen, Y.-C.** (1962) Effective thermal conductivity of ventilated snow. *Journal of Geophysical Research*, **67**(3): 1091-1097.
- Yen, Y.-C.** (1964) Heat transfer by vapor transfer in ventilated snow. *Journal of Geophysical Research*, **68**(4): 1093-1101.

A facsimile catalog card in Library of Congress MARC format is reproduced below.

Yen, Yin-Chao

On the pressure drop through a uniform snow layer / by Yin-Chao Yen.
Hanover, N.H.: U.S. Army Cold Regions Research and Engineering Laboratory; Springfield, Va.: available from National Technical Information Service, 1988.

iv, 17 p., illus.; 28 cm. (CRREL Report 88-14.)

Bibliography: p. 10.

1. Fluid flow. 2. Friction coefficient. 3. Porous media. 4. Pressure.
5. Snow. I. United States Army. Corps of Engineers. II. Cold Regions Research and Engineering Laboratory. III. Series: CRREL Report 88-14.